# Analytical Method for Evaluating Gait Changes Using a Smart Insole: Robot-Induced Effects in a Hemiparetic Patient

Tomoko Funayama
Dept. of Occupational Therapy
Teikyo University of Science.
Yamanashi, Japan
e-mail: funayama@ntu.ac.jp

Yasutaka Uchida
Dept. of Life Science
Teikyo University of Science.
Tokyo, Japan
e-mail: uchida@ntu.ac.jp

Eiichi Ohkubo
Dept. of Life Science
Teikyo University of Science
Tokyo, Japan
e-mail: ohkubo@ntu.ac.jp

Yasunori Fujimori
Dept. of Rehabilitation
Seirei Yokohama Hospital
Kanagawa, Japan
e-mail: yasunori.bb.22@gmail.com

***Abstract*—Wearable devices capable of measuring daily activities have become increasingly accessible, enabling objective assessment in both clinical environments and everyday living settings. Smart insoles integrated into footwear provide continuous and unobtrusive monitoring of plantar loading patterns and are expected to contribute to rehabilitation assessment, including applications involving robotic assistive devices. However, practical challenges remain, such as device design limitations, non-standardized measurement protocols, and the lack of widely accepted evaluation methods. Moreover, gait analysis techniques developed for healthy individuals are often unsuitable for individuals with gait impairments, who typically exhibit atypical or highly variable movement patterns. These issues highlight the need for analytical approaches tailored to impaired gait. This study proposed a novel gait analysis method using a smart insole with embedded pressure sensors in a patient with stroke undergoing inpatient rehabilitation. Smart insole data were collected before, during, and after the use of a gait-assistive robot equipped with a knee–ankle–foot orthosis. Gait data were segmented and analyzed using mean values, temporal parameters, peak-related measures, and insole-pressure distribution, including comparisons of peak counts and visualization of time-series ratios for each insole part. These analyses indicated gait changes associated with robot-assisted walking. This case study demonstrates not only the evaluation of gait changes in a patient with hemiparesis undergoing robot-assisted rehabilitation but also the applicability of a smart insole-based analytical method. To support practical implementation, we present outcome indicators that are easily interpretable for rehabilitation staff.**

***Keywords-gait analysis method; smart insoles; gait-assistive robot; wearable devices; rehabilitation.***

## I. INTRODUCTION

In recent years, the widespread availability of wearable devices capable of measuring daily activities has expanded their use in health-related fields. Wearable devices with high usability expand the scope of assessments that can be conducted not only in specialized environments, such as hospitals and rehabilitation facilities, but also in everyday living settings without altering the usual lifestyle conditions of individuals. Such long-term monitoring capabilities facilitate the detection of subtle changes in health status that may otherwise be overlooked. This approach enables objective assessments not only in therapist-led clinical rehabilitation but also within the patient's home. We have previously conducted research on activity assessment using wearable devices [1, 2].

Among various activities of daily living, gait assessment is one of the most widely used measures because of its strong association with overall functional capacity, risk of falls, and quality of life [3, 4]. It has been applied across a diverse range of patient populations, including older adults [5, 6], individuals with central nervous system disorders (such as cerebrovascular disease, Parkinson disease, and multiple sclerosis) [7–9], patients with cardiovascular and respiratory diseases [10, 11], those with orthopedic conditions such as low back pain [12], individuals with cognitive impairments [13], and various other health conditions. These studies collectively highlight the relevance of gait as a multidimensional clinical indicator capable of reflecting the musculoskeletal, neurological, and cognitive status of individuals. The foot plays a critical role in gait and postural control. It is one of the most sensory-rich regions of the human body and contains numerous receptors that provide continuous feedback essential for maintaining balance and stability. As the foot is the only part of the body that makes direct contact with the ground during an upright stance, it serves as an essential interface for sensing external forces and adjusting posture accordingly. Consequently, alterations in foot loading patterns can offer valuable insights into gait impairment and underlying gait-related conditions.

Insoles are integrated with footwear, and smart insoles equipped with pressure sensors leverage this advantage by enabling continuous, unobtrusive monitoring of plantar loading patterns throughout daily walking episodes. They are also expected to be used for assessment in rehabilitation settings, including robotic assistive devices [14]. Although these devices have substantial potential and an increasing number of studies have reported their utility [15–17], several challenges remain for practical implementation, including issues related to device design, standardization of measurement protocols, and the establishment of universally accepted evaluation methods [18]. Applying gait analysis methods developed for healthy individuals to populations with severe gait impairments may be inappropriate. Individuals with gait impairments may exhibit atypical movement strategies, altered temporal and spatial parameters, or highly variable gait characteristics. Such deviations necessitate analytical frameworks that are specifically tailored to the movement patterns observed in impaired gait rather than relying solely on healthy reference models.

In this context, this study aimed to propose a novel gait analysis method using a smart insole with embedded pressure sensors for a single patient undergoing inpatient rehabilitation following a stroke. The patient participated in rehabilitation involving a gait-assistive robot, and smart-insole data were collected before, during, and after robot use. By analyzing these datasets, we developed an analytical approach designed to detect changes in gait. The robot used in this study was a rehabilitation device attached to a knee–ankle–foot orthosis (KAFO) that assists lower-limb movement by guiding the limb toward a desirable motion pattern during walking.

This case study aimed to demonstrate the feasibility and utility of gait assessment using a smart insole in individuals undergoing rehabilitation and those in need of gait improvement. For practical implementation, the overall picture should be captured. Possessing detailed data alone is insufficient; instead, clear, easily interpretable indicators are required to understand the overall gait characteristics. Therefore, in this study, we presented an analytical method suitable for individuals with gait disorders and proposed outcome indicators that can be easily understood and used by rehabilitation staff.

This study was approved by the Ethics Committee on Research with Humans as Subjects of the Teikyo University of Science. The participant was an individual receiving medical rehabilitation services and was fully informed of the potential benefits and risks of participating in the study. Written informed consent was obtained by occupational therapists from patients undergoing rehabilitation who participated in the study. Section II describes the experimental method, Section III presents the results, Section IV provides a discussion, and Section V concludes the study and outlines future work.

## II. Experimental Methods

A single participant undergoing gait rehabilitation was assessed under three conditions: before, during, and after using the gait-assistive robot. The data were analyzed to develop and propose an analytical method for evaluating the effects of rehabilitation procedures using a gait-assistive robot, that is, changes in gait.

### A. Devices and Software

*1) Smart Insole:* A wireless pressure-sensing smart insole, FEELSOLE® (Toyoda Gosei Co., Ltd), was used in this study. The device was equipped with four pressure sensors positioned at the toe, heel, inside, and outside, enabling measurements at a total of eight points across both feet. A notable characteristic of this insole is its relatively flat structure with minimal slope (Figure 1). The device was calibrated prior to use in the following four steps: (1) no pressure applied without inserting the foot into the shoe; (2) standing with both feet; (3) standing on the left foot only; and (4) standing on the right foot only. The insole sampling frequency was 50 Hz. The insole was connected via Bluetooth to an iOS application, ORPHE TRACK® (ORPHE Inc.), which automatically uploaded the data to the cloud. The recorded data were subsequently downloaded in CSV format using the ORPHE ANALYTICS system for further analysis.

Figure 1. Appearance of the smart insoles.

*2) Gait-Assistive Robot:* In this study, we used the Orthobot® (FINGGAL LINK Inc.), a device used in gait rehabilitation. This device is attached to a KAFO and assists in guiding the lower limb toward a desirable movement pattern during walking. Figure 2 shows a healthy individual wearing the gait-assistive robot.

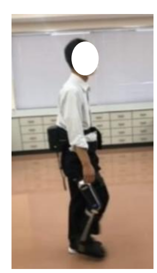

Figure 2. Gait-assistive robot.

### B. Participant and Measurement Method

Gait measurements were conducted on a single male participant in his 70s who was hospitalized and undergoing rehabilitation following a stroke. With the cooperation of the hospital's physical and occupational therapists, gait was assessed under three conditions: before using the gait-assistive robot, during its use, and after its removal. The participant had left hemiparesis and higher brain dysfunction due to a stroke, along with a medical history of traumatic brain injury and left femoral neck fracture. Motor impairments resulting from prior traumatic brain injury were suspected to affect not only the left upper and lower limbs but also the right limbs.

Rehabilitation, including physical, occupational, and speech-language therapies, began the day after stroke onset. Each therapy was provided five times per week, with each session lasting 40 min. Physical therapy included gait training. On day 16 after stroke onset, gait assessment was conducted using the smart insole and gait-assistive robot. As the participant was unable to walk independently, a physical therapist supported the participant from behind during the measurement. The gait-assistive robot was attached to the left lower limb of the participant. The gait tasks included straight walking and a U-turn.

### C. Gait Characteristics and Analysis Method

For the analysis, we excluded the first and last 100 data points recorded at the beginning and end of the measurement period. The raw heel data are shown as the blue line in Figure 3. Our previous study on healthy adults investigated a method for gait assessment using pressure sensor-equipped insoles and suggested the utility of both peak values and post-peak decline rates at the four insole parts during each step [19]. In the present study, the participant's gait was compared with that of healthy controls, and the following distinguishing features were observed: (i) peak and trough values fluctuated and lacked consistency; (ii) peak shapes were irregular, occasionally presenting two successive peaks that produced an "M-shaped" waveform; (iii) the interval between successive heel peaks, that is, the stride time, was inconsistent; (iv) inside and outside pressures on the right foot were reduced; (v) pronounced left–right asymmetry was evident; and (vi) no distinct peaks appeared during periods presumed to correspond to irregular gait while turning.

Because of the wide variation in peak amplitudes, establishing a single threshold for peak detection throughout the entire recording was impractical. Accordingly, the dataset was segmented to exclude intervals with prolonged stride durations, which were assumed to reflect irregular gait. The analysis focused on periods assumed to represent straight walking. The methods used for data segmentation are the following:

*1) Method for Segmenting Insole Data:* The stride-time mode was determined based on the values calculated from the smoothed data. Periods with stride times exceeding 1.1 times the modal duration were considered to involve irregular gait events, such as turning or interruptions, and were excluded from the analysis as non-straight walking. The segmentation procedure involved the following steps:

- Calculation of the modal stride time: Stride duration was calculated from the smoothed data obtained using a moving average with a window size of 11. Stride duration was defined as the interval between the peak value x and the subsequent peak x+1. Peak values were defined as the time points corresponding to the maximum force recorded by the insole sensor at each instance of foot-to-ground contact. Peaks were detected using the find_peaks function in the SciPy Python Library. Equation (1) defines the threshold used to detect peaks in smoothed the data.

$$thresh\_peak = Min + (Max - Min) \times 0.25 \qquad (1)$$

  Subsequently, time bins were created in 0.2-s increments up to the maximum stride duration. Among these bins, the bin containing the highest number of stride durations for the right heel, which was assumed to represent the better-functioning side, was identified, and its upper limit was defined as the modal stride time.
- Exclusion of irregular gait periods: Time intervals exceeding 1.1 times the modal stride duration was regarded as irregular gait, such as during turning or interruptions, and were excluded from the analysis to isolate segments representing straight walking. To ensure that the start and end times of the straight walking segments did not overlap with any of the peak values, a buffer equal to one-fourth of the median stride time of the right heel (calculated after smoothing) was added to both ends of each segment. The longest straight walking segment was used for further analysis.

*2) Peak Characteristics of Raw and Moving-Average Insole Data:* Compared with cases without gait impairment, this case exhibited non-normal peak patterns characterized by consecutive double peaks, forming an M-shaped waveform. Therefore, two types of peak values were calculated: peaks derived from the raw insole data and those derived from data smoothed using a moving average with a window size of 11. The number of peaks and mean values were examined. To extract gait instability, the peak characteristics from the raw data and moving-average data were compared.

*3) Calculation of Mean Values:* The mean values for each insole part were calculated using both non-segmented and segmented raw data, and the resulting mean values were compared between the two datasets.

*4) Mean of Peak Values:* For non-segmented and segmented data, the peak values were defined as the maximum force detected at the heel, toe, inside, and outside parts of the insole during each instance of foot-to-ground contact.

*5) Decline Rates and Classification Feasibility:* The decline rate reflects the decrease in pressure values following each peak. To investigate the feasibility of classifying gait patterns before and after robot-assisted walking, support vector machine (SVM) analyses were performed using the maximum decline rates of heel and toe insole data from both the segmented and non-segmented datasets. Because this study was based on a single clinical case with a limited dataset, the SVM analysis was conducted as an exploratory feasibility evaluation rather than a comprehensive machine-learning performance comparison.

- Calculation of Decline Rate: The decline rate reflects the decrease in pressure values following each peak. In this study, it was calculated by measuring the difference in the weighted averages between adjacent data points. Specifically, the decline rate was defined as the difference between the weighted averages at points x and x+1. The weighted average was calculated using five consecutive data points: the target, two preceding points, and two succeeding points. To emphasize the influence of the central value, weights were assigned as follows: 40% to the target point, 20% to the points immediately before and after, and 10% to the secondary points before and after. Among the calculated decline rates, the largest value within each foot-to-ground contact was defined as the maximum decline rate. The maximum values were extracted for each instance, and the mean values were computed.
- Feasibility of the SVM-based classification: To explore the feasibility of classification using a SVM based on the decline rate of insole data, we examined the classification of the data when the maximum decline rate at each sole-to-ground contact was used as supervised data. As an initial stage of investigating a classification method, we assessed how supervised data could be categorized and considered the potential applicability of SVM-based classification. For "right heel and right toe" and "left heel and left toe" before and after robot use, SVM analyses were conducted using four types of datasets: non-segmented and segmented data. To ensure a one-to-one correspondence between the heel and toe values, the average values were calculated when continuous data such as 1-to-2 or 2-to-1 pairs occurred. SVM analysis was implemented using the scikit-learn library in Python, employing the svm module and SVC class. The SVM parameters were set as follows: C = 100.0, kernel = rbf, and gamma = 0.001. These parameters were selected to avoid overfitting while ensuring appropriate model complexity, and the same parameter set was applied to all analyses. The dataset was split into training and test sets using the train_test_split function with a fixed random_state of 42, allocating 80% and 20% of the data for training and testing, respectively.

*6) Calculation of Sole Contact Time and Stride Time:* The analysis was conducted using the segmented dataset with the longest walking duration after excluding periods of irregular gait.

- Calculation of Sole Contact Time
  In this case, peak and valley values varied substantially, making it difficult to define a single threshold applicable to the entire walking dataset. Therefore, the threshold for detecting sole contact in this case was modified and determined using the extracted peak and valley values. The thresholds for peak and valley extraction were defined by Equations (2) and (3), respectively. The sole contact threshold was then calculated using the median values of the extracted peaks and valleys, as shown in Equation (4). The median was used instead of the mean to reduce the influence of extreme values. If sole contacts were not alternately detected between the left and right sides, and two or more consecutive sole contacts were detected on the same side, these were merged into a single sole contact event. Specifically, the durations of consecutive detections were summed, and the sensor values were averaged.

$$peak\_thresh = Min + (Peak\_ave - Min) \times 0.2 \tag{2}$$

$$valley\_thresh = Min + (Max - Min) \times 0.4 \tag{3}$$

$$Sole\_contact\_thresh = valley\_median + (peak\_median - valley\_median) \times 0.3 \tag{4}$$

- Calculation of stride time: Since peak values occasionally appeared in rapid succession and irregular forms, a moving average was applied to smooth the data and calculate stride times. The signal was smoothed using a moving average with a window size of 11. The stride time was defined as the interval between two successive heel peaks on the same side (left or right).

*7) Insole Part Proportions and Time-Series Changes*: The proportion of loading in the heel, toe, inside, and outside parts relative to the total insole load was calculated, and a color-coded time-series graph was generated to visualize the pressure characteristics for each insole part. Because the left and right data were recorded alternately, simultaneous bilateral measurements at the same time points were not possible. Therefore, for the right side, the mean of two consecutive values was regarded as corresponding to the same time point as the left side data and was used for the analysis. Visualizing the time-series changes in the load distribution across the insole parts facilitated a clear understanding and improved interpretability. This approach enabled comprehension beyond numerical values alone and suggested potential applicability in clinical settings.

## III. RESULTS

### A. Data Segmentation

Among the walking periods, excluding irregular segments, the longest and second-longest durations were identified, and the longest was used for the analysis. To avoid overlap with the peak values, one-fourth of the median right-heel stride time was added to both ends. Figure 3 shows the walking data before, during, and after robot use. The green lines indicate the start times of the segments estimated as straight walking, and the yellow lines indicate their end times. Irregular gait was removed before robot use; however, after removal, some irregular segments were misclassified as straight walking. While the robot was worn, a small portion of irregular gait was also included.

### *B. Mean Values*

Figure 4 shows the mean values of the segmented and non-segmented data, with some differences despite similar overall trends. Specifically, the mean value for the right heel after robot removal was lower in the segmented data than in the non-segmented data, and the left–right asymmetry was reduced. Additionally, the mean value of the right toe increased after robot removal. In the figures and tables, the terms “non-split” and “split” indicate non-segmented and segmented data, respectively.

### *C. Comparison of Peak Counts Between Raw and Moving-Average Insole Data*

A comparison graph of the number of peaks extracted from the non-segmented and segmented datasets is shown in Figure 5 and a summary of the peak counts, mean values, and median values is provided in Table I. Only the right-side segmented data during robot use showed the same number of peaks between the raw and moving-average data. In all other conditions, the raw data contained more peaks. Compared with the non-segmented data, the segmented data showed smaller differences between the raw and moving-average results, except for the left heel before robot use. Because the moving average used a window size of 11, peaks occurring immediately after the start or just before the end of the interval were smoothed out and often not detected, resulting in one to two fewer peaks. Even when considering this reduction, the segmented data still showed smaller discrepancies than the non-segmented data. For the segmented left-heel data, which showed the largest discrepancy, Figure 6 presents the raw and moving-average data before and after robot use. The red arrows indicate the extracted peak points. Before robot use, multiple peaks occurred within a single-foot contact phase, whereas after removal, each contact produced a single peak, resulting in a more regular waveform.

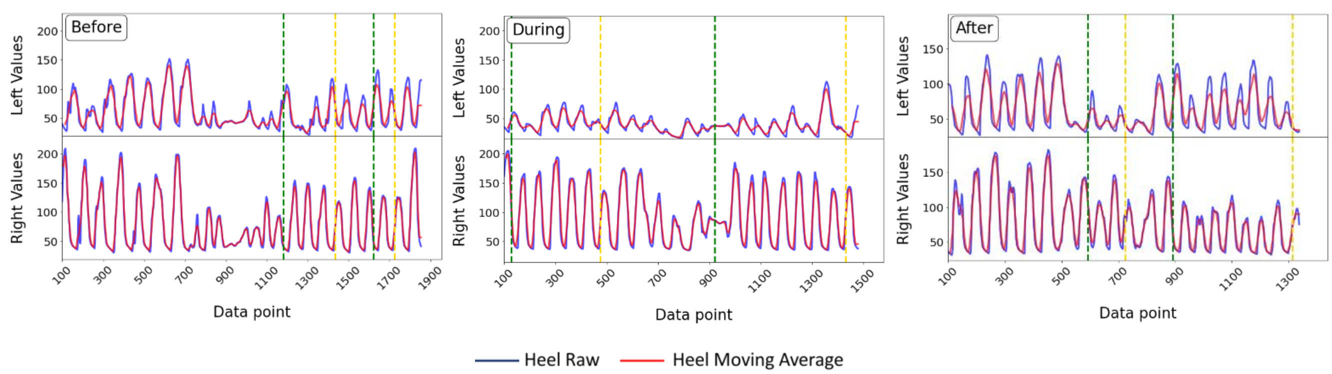


Figure 3. Irregular walking exclusion time.

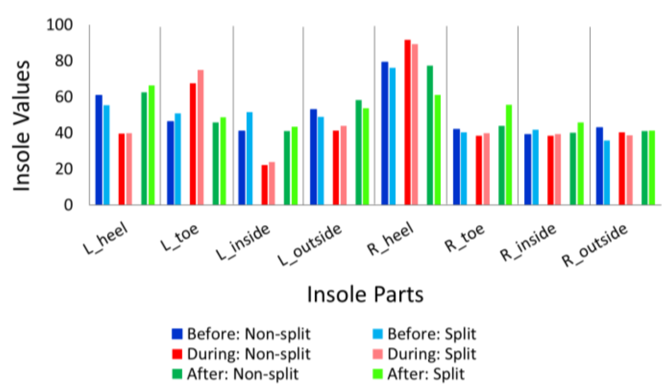


Figure 4. Mean values of insole parts from split and non-split data.

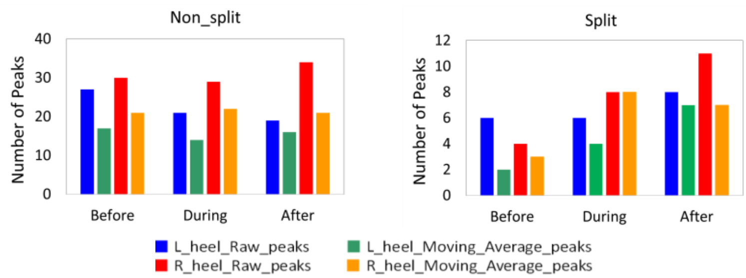


Figure 5. Heel peak counts in split and non-split data.

TABLE I. PEAK COUNT, MEAN, AND MEDIAN OF RAW AND MOVING AVERAGE IN NON-SPLIT AND SPLIT DATA.

| Division / Left , Right / Stats , Implementation | | Heel_peaks : Non_split | | | | | |
|---|---|---|---|---|---|---|---|
| | | L_Raw | L_Moving_Average | L_Ratio | R_Raw | R_Moving_Average | R_Ratio |
| count | Before | 27 | 17 | 1.59 | 30 | 21 | 1.43 |
| | During | 21 | 14 | 1.50 | 29 | 22 | 1.32 |
| | After | 19 | 16 | 1.19 | 34 | 21 | 1.62 |
| mean | Before | 101.63 | 94.99 | 1.07 | 143.84 | 142.04 | 1.01 |
| | During | 57.86 | 56.58 | 1.02 | 151.02 | 147.01 | 1.03 |
| | After | 110.55 | 93.98 | 1.18 | 116.76 | 118.65 | 0.98 |
| median | Before | 102.32 | 98.00 | 1.04 | 143.90 | 142.63 | 1.01 |
| | During | 50.80 | 53.02 | 0.96 | 162.20 | 154.91 | 1.05 |
| | After | 112.64 | 90.68 | 1.24 | 110.18 | 116.34 | 0.95 |
| Division / Left , Right / Stats , Implementation | | Heel_peaks : Split | | | | | |
| | | L_Raw | L_Moving_Average | L_Ratio | R_Raw | R_Moving_Average | R_Ratio |
| count | Before | 6 | 2 | 3.00 | 4 | 3 | 1.33 |
| | During | 6 | 4 | 1.50 | 8 | 8 | 1.00 |
| | After | 8 | 7 | 1.14 | 11 | 7 | 1.57 |
| mean | Before | 76.00 | 82.49 | 0.92 | 149.41 | 142.86 | 1.05 |
| | During | 64.38 | 63.29 | 1.02 | 154.89 | 146.71 | 1.06 |
| | After | 107.10 | 82.34 | 1.30 | 94.69 | 92.38 | 1.03 |
| median | Before | 67.67 | 82.49 | 0.82 | 148.93 | 143.76 | 1.04 |
| | During | 53.63 | 54.69 | 0.98 | 165.94 | 152.36 | 1.09 |
| | After | 110.25 | 82.10 | 1.34 | 93.32 | 94.64 | 0.99 |

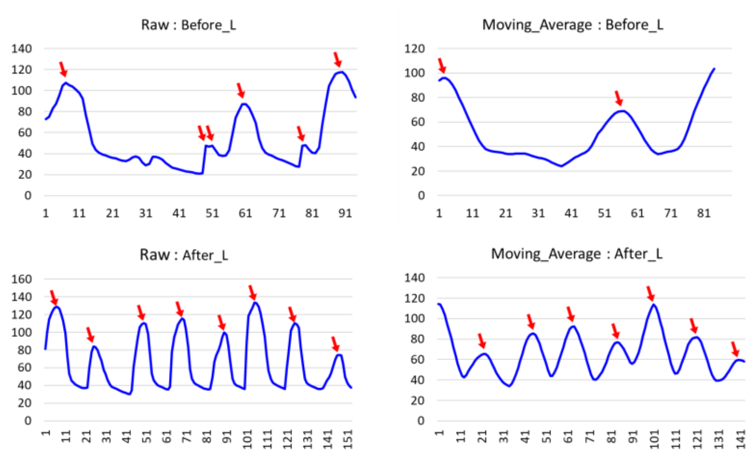


Figure 6. Peaks in raw and moving-average data by split.

### D. Mean Peak Values

The mean peak values for each insole part are shown in Figure 7. These results show trends similar to those shown in Figure 4, which presents the mean values for the full raw dataset. After robot use, peak values at the left heel and outside—the side with the robot—increased compared with before use. On the right side, without the robot, heel peak values decreased, reducing asymmetry, whereas toe peaks increased.

### E. Decline Rate

The mean absolute values of the maximum decline rates for each insole part are shown in Figure 7, and a comparison of the mean values before and after robot removal shows higher overall rates after removal. On the left side, the segmented data showed a slight decrease in the inside part but increases elsewhere, with a particularly large change at the left heel. On the right side, the decline rate decreased at the heel but increased in other parts, especially at the toe. These findings suggest that robot-assisted walking led to a higher rate of change per unit time, particularly on the side where the robot was worn.

### F. SVM Classification Using Maximum Decline Rates

For the heel and toe on both the right and left sides before and after robot use, SVM analyses were performed using non-segmented and segmented datasets. The results are shown in Figure 8. The classification accuracy was higher for the segmented data than for the non-segmented data and was also higher for the right side, the functionally better, non-robot-assisted limb, than for the robot-assisted left side. Although differences in sample size may have influenced these results, the scatter plots indicated that segmented data provided clearer separability. When all data were used for training, the accuracy for the left (robot-assisted) side was 65.9% for the non-segmented data and 90.9% for the segmented data, whereas the right side showed accuracies of 72.7% and 100%, respectively. When 80% and 20% of the data were used for training and testing, respectively, the accuracies for the left side were 55.6% (non-segmented) and 33.3% (segmented), whereas those for the right side were 66.7% (non-segmented) and 100% (segmented). Black points indicate data before robot-assisted walking, and red points indicate data after robot-assisted walking.

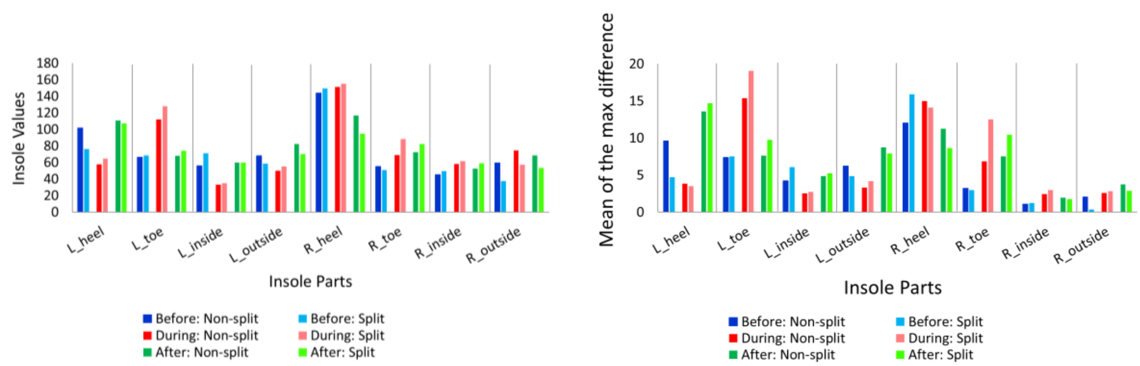


Figure 7. Mean peak values (left) and decline rates (right) for each insole part.

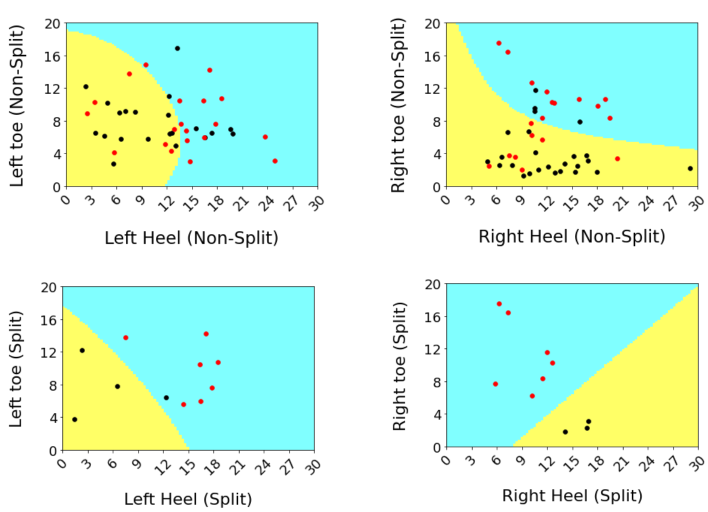


Figure 8. SVM classification of heel and toe decrease using split and non-split data.

### G. Insole Part Proportions and Time-Series Changes

Time-series graphs were generated to visualize changes in the proportional load distribution across each part of the insole. As shown in the earlier overall raw data plot in Figure 9, there was no substantial difference before and after wearing the robot; the proportion of the right heel decreased only slightly after removal compared with before use. However, the time-series graphs revealed that the loading pattern on the right heel had changed. Furthermore, the proportion at the right heel was lower and the proportion at the toe was higher in the latter half of walking after robot removal than in the first half.

### H. Sole Ground Contact Time

The results for the mean sole contact time are shown in Figure 10. After walking with the robot, sole contact time decreased across all insole parts. Before robot use, the sole contact time on the left medial side was longer than that on the left outside; however, after robot removal, the outside exhibited longer contact times than the medial side. Changes were observed between the inside and outside parts on the left side, as indicated by the comparison presented here, highlighting variations that became more apparent through this analysis of the segmented data.

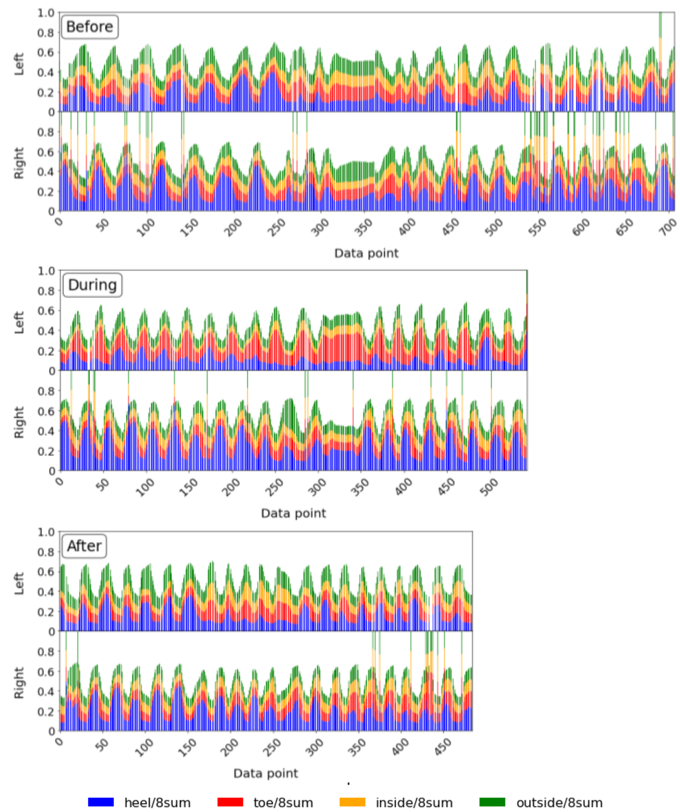


Figure 9. Proportions and temporal changes in insole parts.

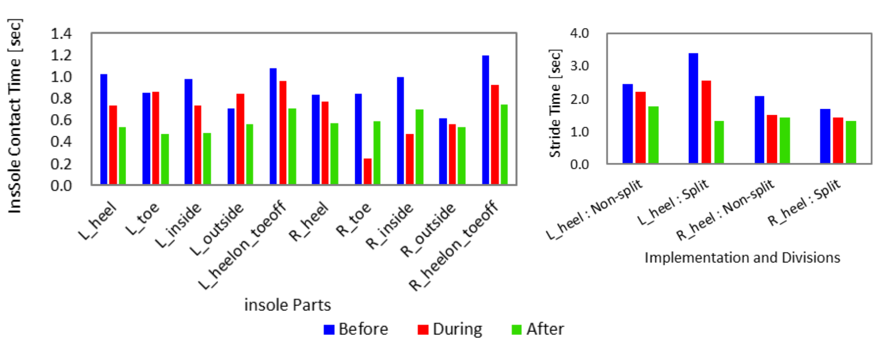


Figure 10. Ground contact time (left) and stride time (right).

### I. Stride Time

The mean stride time results are shown in Figure 10. Compared with the functionally better right side, the left side tended to exhibit longer stride times. After robot removal, stride time decreased overall, and left–right differences in stride time were reduced. However, large discrepancies were observed between segmented and non-segmented data for the left heel. Regarding left–right differences, the segmented data showed larger asymmetry than the non-segmented data, particularly before robot use. Examination of the raw data graphs shown in Figure 3 revealed substantial left–right differences, even during periods that appeared to correspond to straight walking before and during robot use. Raw data graphs also indicated marked left–right differences even during periods that appeared to be straight walking, consistent with the trends observed in the segmented stride times derived from (2)–(4). However, the segmented dataset contained few sole-contact events; before robot use, the left-side stride time could be calculated only once or twice. Therefore, although the segmented stride time served as an indicator of gait tendencies, it was not possible to conclusively determine that these data fully represented the gait characteristics, including left–right asymmetry.

## IV. Discussion

The participant in this study, who had gait impairments, had more irregular walking data than healthy individuals; thus, the same analytical approach could not be applied. Irregular periods were therefore excluded, and the data were segmented. To avoid distortion from extremely long or short stride durations, stride time was represented using the mode, and periods exceeding 1.1 times the modal value were treated as irregular walking. Although a lower threshold excludes irregular intervals more strictly, it risks removing valid straight walking data. Furthermore, these parameters may vary with gait speed and balance, requiring settings that prioritize assessment items. Segmentation effectively removed irregular walking before robot use; however, some irregular data remained during and after use. The better-functioning right limb showed more regularity, whereas the left limb retained irregularity, suggesting that segmentation based on both limbs, and not only the better-functioning side, may be useful. The usefulness of the segmented data was suggested by the results for peak values, maximum decline rates, stride time, and exploratory SVM classification. In terms of stride time, segmented data also showed greater left–right asymmetry than non-segmented data, particularly before robot use, consistent with trends observed in the raw data graphs. These findings indicate that the characteristics of straight walking were likely captured in the segmented data. However, the number of detected foot contacts was limited, indicating that additional usable segments beyond the longest one may be required for reliable characterization. Although the walking duration was short and the amount of gait data was limited in the present study, future studies using longer walking periods and larger amounts of gait data may enable the application of advanced classifier fusion and regularization approaches [20]. Additionally, this study examined only straight walking, whereas prior work has emphasized the importance of turning movements in fall-risk assessment [21]. This points to the need for future analyses incorporating irregular gait phases and refining segmentation methods to gain further insights.

We compared the peak counts obtained from the raw data with those from the moving-average-filtered data to evaluate gait stability. The difference in peak counts between the two datasets indicates that this approach is effective for identifying instability. Given a sampling frequency of 50 Hz and a window size of 11, the moving average was calculated over 0.22-s intervals. For individuals with slower gait speeds, a larger window size may be required to appropriately capture their movement characteristics. Therefore, the optimal window size should be determined by considering both gait speed and sampling frequency to ensure accurate assessment for each participant.

The time-series graphs of pressure distribution ratios across the insole parts effectively captured temporal changes in loading that were difficult to discern from the raw data alone. The ability to easily grasp loading changes and trends makes this visualization highly beneficial for clinical rehabilitation and daily gait assessment. In the latter half of the walking phase after removal, the proportion of loading on the right heel decreased, whereas that on the toes increased. This indicates that loading patterns differ between the early and late stages of walking, implying that gait training may require adjustments such as incorporating rest breaks in response to unfavorable patterns or encouraging continued walking when desirable responses are observed. Furthermore, analyzing loading ratios may reflect changes in lower-limb muscle tone, thereby guiding orthotic adjustments. Therefore, time-series loading ratio graphs have strong potential to inform the design of individualized gait training strategies. No matter how high the technical accuracy, data are difficult to use if healthcare professionals cannot easily operate and interpret them. High precision and large volumes of data alone do not necessarily lead to practical usefulness. Success in a clinical context depends not only on providing extensive, high-precision data but also on ensuring that the data are actionable for the end-user. A survey investigating clinical expectations for smart insoles used in knee osteoarthritis care presented the view of healthcare professionals that data should be provided in an easily interpretable format, with the option of accessing more detailed information when needed [22]. The time-series pressure distribution graph is considered to fulfill this requirement as a useful, summarized data format. Although the investigation involved indoor walking in a hospital, daily life gait assessment has been reported to detect condition changes earlier [23], suggesting its usefulness in real-life settings. Outdoor walking is affected by differences in surface and slope [24]; therefore, further investigation is required.

## V. Conclusions and Future work

In this study, gait data were segmented and analyzed through mean-value calculations, temporal parameters, peak-related measures, and insole pressure distribution, including comparisons of peak counts and visualization of time-series ratios for each insole part. These analyses captured the changes in gait improvement resulting from robot-assisted walking. As this was a single-case study, the generalizability of the results is limited. Future studies should include a larger sample size and further investigate the measurement data, analysis methods, and insole design.

## ACKNOWLEDGMENTS

We express our sincere gratitude to the patient and hospital staff who participated in this study. This study was supported by the JSPS KAKENHI (grant number JP23K11207).

## REFERENCES

[1] T. Funayama, Y. Uchida, E. Ohkubo, and R. Kimura, "Segmented Gait Analysis Using Pressure-Sensing Insoles in a Hemiparetic Patient: a Case Study," Global Health 2025, pp. 18-23, 2025.

[2] T. Funayama, Y. Uchida, E. Ohkubo, and Y. Kogure, "Exploring the Potential of a Wrist-Worn Optical Sensor for Measuring Daily Life Activities," Global Health 2023, pp. 18-24, 2023.

[3] A. S. Alharthi, S. U. Yunas, and K. B. Ozanyan, "Deep learning for monitoring of human gait: a review," IEEE Sensors Journal, vol. 19, No. 21, pp. 9575–9591, 2019.

[4] V. Bucinskas et al., "Wearable feet pressure sensor for human gait and falling diagnosis," Sensors, vol. 21, issue 15, 5240, 2021, doi: 10.3390/s21155240.

[5] N. Takayanagi, M. Sudo, Y. Yamashiro, I. Chiba, S. Lee, Y. Niki, and H. Shimada, "Predictivity of daily gait speed using tri-axial accelerometers for two-year incident disability among Japanese older adults," Scientific Reports, vol. 12, 10067, 2022, doi: 10.1038/s41598-022-14304-9.

[6] I. Bytyçi and M. Y. Henein, "Stride length predicts adverse clinical events in older adults: a systematic review and meta-analysis," Journal of Clinical Medicine, vol. 10, issue 12, 2670, 2021, doi: 10.3390/jcm10122670.

[7] L. Angelini et al., "Wearable sensors can reliably quantify gait alterations associated with disability in people with progressive multiple sclerosis in a clinical setting," Journal of Neurology, vol. 267, pp. 2897–2909, 2020, doi: 10.1007/s00415-020-09928-8.

[8] C. J. Hass et al., "Quantitative normative gait data in a large cohort of ambulatory persons with Parkinson's disease," Plos One, vol. 7, issue 8, e42337, 2012, doi: 10.1371/journal.pone.0042337.

[9] D. M. Mohan, A. H. Khandoker, S. A. Wasti, S. I. I. I. Alali, H. F. Jelineki, and K. Khalaf, "Assessment methods of post-stroke gait: a scoping review of technology-driven approaches to gait characterization and analysis," Frontiers in Neurology, vol. 12, 650024, 2021, doi: 10.3389/fneur.2021.650024.

[10] K. Kamiya et al., "Gait speed has comparable prognostic capability to six-minute walk distance in older patients with cardiovascular disease," European Journal of Preventive Cardiology, vol. 25, issue 2, pp. 212–219, 2018, doi: 10.1177/2047487317735715.

[11] G. Fischer et al., "Factors influencing self-selected walking speed in fibrotic interstitial lung disease," Scientific Reports, vol. 11, 12459, 2021, doi: 10.1038/s41598-021-91734-x.

[12] A. Demirel, D. Onan, M. Oz, Y. O. Aslıyuce, and O. Ulger, "Moderate disability has negative effect on spatiotemporal parameters in patients with chronic low back pain," Gait & Posture, vol. 79, pp. 251–255, 2020, doi: 10.1016/j.gaitpost.2020.05.015.

[13] Y. C. Kuan et al., "Balance and gait performance in older adults with early-stage cognitive impairment," European Journal of Physical and Rehabilitation Medicine, vol. 57, issue 4, pp. 560 - 567, 2021, doi: 10.23736/S1973-9087.20.06550-8.

[14] L. D'Arco, H. Wang, and H. Zheng, "Integration of smart insoles for gait assessment in exoskeleton assisted rehabilitation," Scientific Reports, vol. 15, 28350, 2025, doi: 10.1038/s41598-025-10032-y.

[15] V. Tsakanikas et al., "Evaluating gait impairment in Parkinson's disease from instrumented insole and IMU sensor data," Sensors, vol. 23, issue 8, 3902, 2023, doi: 10.3390/s23083902.

[16] S. Subramaniam, S. Majumder, A. I. Faisal, and M. J. Deen, "Insole-based systems for health monitoring: current solutions and research challenges," Sensors, vol. 22, Issue 2, 438, 2022, doi: 10.3390/s22020438.

[17] B. Park, M. Kim, D. Jung, J. Kim, and K. R. Mun, "Smart insole-based abnormal gait identification: deep sequential networks and feature ablation study," Digital Health, vol. 11, 2025, doi: 10.1177/20552076251332.

[18] V. M. Santos, B. B. Gomes, M. A. Neto, P. F. Rodrigues, and A. M. Amaro, "A systematic review on smart insole prototypes: development and optimization pathways," Actuators, vol. 14, issue 8, 408, 2025, doi: 10.3390/act14080408.

[19] T. Funayama, Y. Uchida, Y. Kogure, D. Souma, and R. Kimura, "Exploring the assessment of steps using insoles with four-part pressure sensors," Sensors & Transducers, vol. 263, issue 4, pp. 21–28, 2023.

[20] A. Salazar, L. Vergara, G. Safont, and E. Vidal, "Graph regularization methods for soft detector fusion," IEEE Access, vol. 11, pp. 144747–144759, 2023, doi: 10.1109/ACCESS.2023.3344776.

[21] J. M. Leach, S. Mellone, P. Palumbo, S. Bandinelli, and L. Chiari, "Natural turn measures predict recurrent falls in community-dwelling older adults: a longitudinal cohort study," Scientific Reports, vol. 8, 4316, 2018, doi: 10.1038/s41598-018-22492-6.

[22] D. Lin, E. Papi, and A. H. McGregor, "Exploring the clinical context of adopting an instrumented insole: a qualitative study of clinicians' preferences in England," BMJ Open, vol. 9, e023656, 2019, doi: 10.1136/bmjopen-2018-023656.

[23] E. Warmerdam, C. Wolff, M. Orth, T. Pohlemann, and B. Ganse, "Long-term continuous instrumented insole-based gait analyses in daily life have advantages over longitudinal gait analyses in the lab to monitor healing of tibial fractures," Frontiers in Bioengineering and Biotechnology, vol. 12, 1355254, 2024, doi: 10.3389/fbioe.2024.1355254.

[24] E. Warmerdam, L.-M. Burger, D. F. Mergen, M. Orth, T. Pohlemann, and B. Ganse, "The walking surface influences vertical ground reaction force and centre of pressure data obtained with pressure-sensing insoles," Frontiers in Digital Health, vol. 6, 1476335, 2024, doi: 10.3389/fdgth.2024.1476335.